



Sequence Stratigraphic Framework of the Jurassic Samana Suk Carbonate Formation, North Pakistan: Implications for Reservoir Potential

Bilal Wadood^{1,2} · Suleman Khan³ · Hong Li¹ · Yiqun Liu¹ · Sajjad Ahmad^{3,4} · Xin Jiao¹

Received: 16 February 2020 / Accepted: 17 May 2020 / Published online: 3 June 2020
© King Fahd University of Petroleum & Minerals 2020

Abstract

The paper aims to establish a possible link between the sequence stratigraphy and reservoir potential of the Middle Jurassic carbonates of Samana Suk Formation, Kala Chitta Range, North Pakistan. The Samana Suk Formation is comprised of a monotonous sequence of thin- to thick-bedded bioturbated, cross-bedded, ripple marked, sandy, bioclastic carbonates with shale interbeds. The rock unit is the best analog of shallow to marginal marine carbonates due to its pronounced thickness, enhanced lithological variations, and diverse diagenetic features. To establish a possible link between the sequence stratigraphy and reservoir potential of the rock unit, the outcrop and petrographic features are used to record eight microfacies, deposited in a wide range of shallow to marginal marine environments including mudflats, lagoon, back shoals, and sand shoals. Based on the vertical stacking pattern of microfacies in a given time of deposition (170–160 Ma), one second-order local cycle (SLC-1), three regressive systems tracts (RSTs) and two transgressive systems tracts (TSTs) are delineated within the succession. The primary and secondary porosity of selected microfacies from each systems tracts are investigated using petrography, scanning electron microscopy, and energy-dispersive spectroscopy. The direct measurements of porosity and permeability of these microfacies types are carried out using high overburden pressure plug porosity and permeability analyses. Based on these investigations, higher reservoir potential is recorded for mudstones/wackestone microfacies of RST as compared to grainstone microfacies of TST. The higher porosity within RST and higher interconnectivity of available pores both in RST and in TST suggest that the Samana Suk Formation carries good reservoir potential.

Keywords Jurassic · Carbonates · Microfacies · Sequence stratigraphy · Reservoir

1 Introduction

This paper investigates a possible link between the sequence stratigraphy and reservoir potential of the shallow to marginal marine carbonates of the Middle Jurassic Samana Suk

Formation, Kala Chitta Range, North Pakistan (Fig. 1). It has been established that the primary and secondary porosity within the carbonate rocks can be linked with transgressive/regressive cycles [1, 2]. During regression, the larger inter-/intra-particles interconnected pores are usually filled

✉ Yiqun Liu
liu-yiqun@263.net

Bilal Wadood
bilalwadood@uoswabi.edu.pk

Suleman Khan
sulemanafriidi@uop.edu.pk

Hong Li
lihong2008@nwu.edu.cn

Sajjad Ahmad
dr.s_ahmed@uop.edu.pk

Xin Jiao
jxin807@163.com

¹ State Key Laboratory of Continental Dynamics, Department of Geology, Northwest University, Xi'an 710069, China

² Department of Geology, University of Swabi, Swabi 23561, Pakistan

³ Department of Geology, University of Peshawar, Peshawar 25120, Pakistan

⁴ Department of Earth and Atmospheric Sciences, University of Houston, Houston 77004, USA



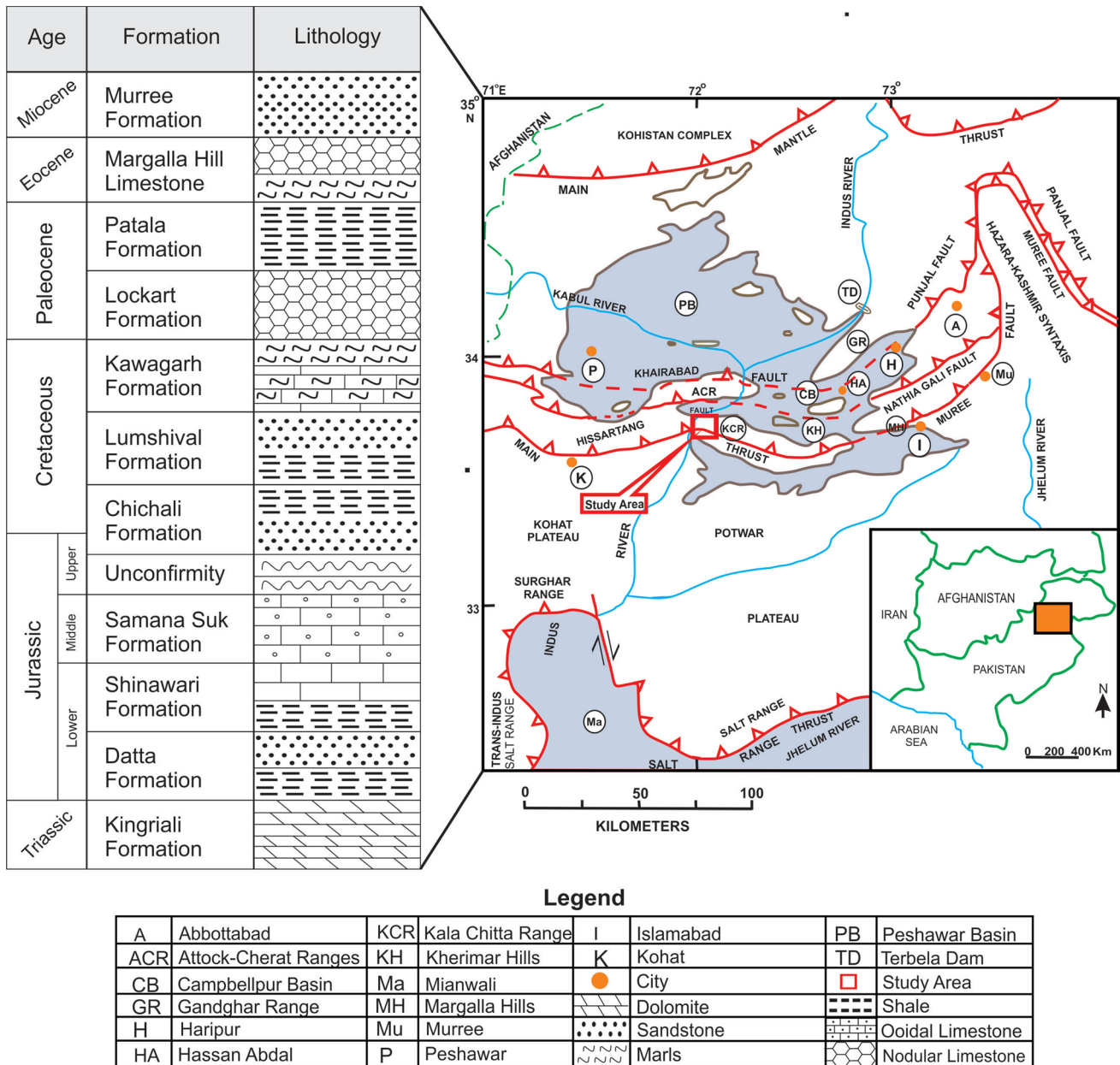


Fig. 1 Generalized tectonic and structural map of the study area [32] and stratigraphic log of the Kala Chitta Range, North Pakistan

by heavy cementation, which subsequently occludes the primary porosity [1, 3, 4]. Conversely, during transgression, the deposition of matrix-supported carbonates preserves higher primary porosity [1]. However, in marginal marine carbonate system, the regression results in the development of protected environments of proximal settings (i.e., lagoon and tidal flats) [1]. Such depositional environments are characterized by mudstone–wackestone microfacies with relatively higher porosity than offshore grainstone microfacies associated with marine transgression [4, 5]. The diagenesis-induced secondary porosity in carbonate rocks can also be affected by sea-level changes [5]. The pore-water chemistry

of near-surface (marine), hypersaline (intertidal, supratidal, lagoon), brackish (delta and estuary), and meteoric (continental) depositional environments varies drastically [2, 4, 6–8]. The sea-level fluctuations bring changes in the pore-water chemistry of carbonate sediments by changing the chemistry near the sediments/water interface [5]. The transgressive/regressive cycles also determine the residence time of a diagenetic process and hence the extent of diagenetic alterations. Low sedimentation rates during transgression result in prolonged exposure of sediments to marine pore-water diagenesis, whereas the prolonged subaerial exposure of carbonate sediments during regression results in extensive

meteoric diagenesis [5]. The changes in sea level also cause changes in the size and proportion of carbonate grains [2, 5, 7]. The composition of grains controls their mechanical and chemical properties and hence susceptibility to particular diagenesis [5]. Furthermore, the sea-level changes affect the amount and type of organic matter [9, 10] which in turn controls the dissolution of the carbonate matrix as a result of organically produced methane exhalation [1]. By now, it is evident that sequence stratigraphy controls both primary and secondary diagenetic porosity [11, 12]. Therefore, linking sequence stratigraphy, primary porosity, and secondary diagenetic porosity of the shallow to marginal marine carbonates may act as a robust tool for the evolution of porosity and permeability in carbonate rocks and hence their reservoir potential [5]. To establish a possible link between the sequence stratigraphy and reservoir potential of shallow to marginal marine settings, the carbonates of Samana Suk Formation are investigated in the present study.

The Samana Suk Formation hosts frequent variations in its carbonate lithologies and diagenetic features. Based on these characteristics, the Samana Suk Formation is the best analog of shallow to marginal marine carbonates and hence suitable for this study. The formation is comprised of thin- to thick-bedded limestone with minor intercalations of shales. Previously, it is investigated in detail by various researchers for its sedimentology, paleontology, and stratigraphy attributes [13–25]. The microfacies and diagenetic analyses of the Samana Suk Formation are carried out in Surghar Range, Trans Indus Ranges, to establish the depositional environment and diagenetic sequence of the studied section [21]. It is suggested that the rock unit is deposited in inner to outer shelf with open to restricted conditions [21]. In addition, Hussain et al. [26] documented microfacies and diagenetic details in a 60-m-thick section of the Samana Suk Formation in Harnoi section, District Abbottabad, Pakistan. They documented inner to mid-ramp depositional environment for the formation. They also observed various diagenetic features including the varying degree of late-stage dolomitization at different stratigraphic intervals. Ali et al. [27] established the depositional environment and sequence stratigraphy of the Samana Suk Formation in Chichali Nala, Trans Indus Ranges, Pakistan. They documented near shore to beach, lagoonal, barrier shoal, and deeper subtidal ramp environments for the deposition of the unit (50 m). They also documented two second-order and four third-order sequences. Hayat et al. [28] documented microfacies-based sequence stratigraphy for a 13-m-thick section in the Namal Gorge, Salt Range, Upper Indus Basin. They established one second-order and two-third-order sequences within the unit. Other researchers focused on the dolomites of the Samana Suk Formation, investigating the fault-controlled parallel-bedded dolomite of the unit in the Hazara basin, NW Pakistan [29]. They concluded that the dolomitization

in the studied section is controlled by the percolation of Mg-rich fluids through a local fault. Furthermore, Shah et al. [29] documented that the late-stage dolomitization is pronounced in mudstone to wackestone microfacies as compared to grainstone microfacies of the Samana Suk Formation in southern Hazara Basin, NW Himalayan Fold and Thrust belt. Their study also concluded that the less porous/permeable mudstone microfacies evolved into more pore/permeable facies as a result of dolomitization.

It is evident from the literature review that previously the Samana Suk Formation is studied in detail in the context of depositional environment, sequence stratigraphy, and diagenetic history. However, work on the development and modification of porosity in connection with sequence stratigraphy is still lacking. This paper integrates the outcrop and petrographic details for establishing a sound sequence stratigraphic framework of the unit. In this study, we evaluate the reservoir potential of various systems tracts, using petrography, scanning electron microscopy (SEM), energy-dispersive X-ray spectroscopy (EDX), high overburden pressure plug porosity/permeability, and production recovery rates of selected microfacies.

2 Geological Setting

Tectonically, the studied section is part of the Kala Chitta Range (KCR), North Pakistan (Fig. 1). Regionally, KCR represents the northwest margin of the Indian Plate (Fig. 1). It is an integral part of the Himalayan foreland folds and thrusts. The closure of Tethys, the continent–continent collision between India and Asia, and formation of Main Mantle Thrust (MMT) at about 55–50 Ma mark the initiation of the Himalayan foreland fold and thrust belts [30–34]. The formation of MMT is succeeded by the emplacement of regional continental thrusts, i.e., the Main Boundary Thrust (MBT) and the Main Frontal Thrust (Salt Range Thrust in Pakistan), as a result of southward propagation of transport direction [35]. Due to the successive uplift along the MBT and Salt Range Thrust (SRT), important geomorphic features like KCR and the Salt Range are formed, respectively (Fig. 1). In addition, the intervening plains between these ranges are uplifted as Potwar and Kohat Plateaus (Fig. 1). The intermountain basins [i.e., Peshawar (PB) and Campbellpore (CB)] in the north of the study area are formed as a result of uplift along the Attock Cherat Range (ACR) (Fig. 1). The study area is bounded in the north by the prominent Khairabad and Hissartang thrust faults, which have exposed Pre-Cambrian to Paleozoic meta-sedimentary/sedimentary sequence along the ACR. The uplift along Khairabad and Hissartang Faults is pre- to syn-Himalayas [32, 36]. The stratigraphic studied section is part of KCR which is uplifted along the MBT. The MBT is a regional thrust

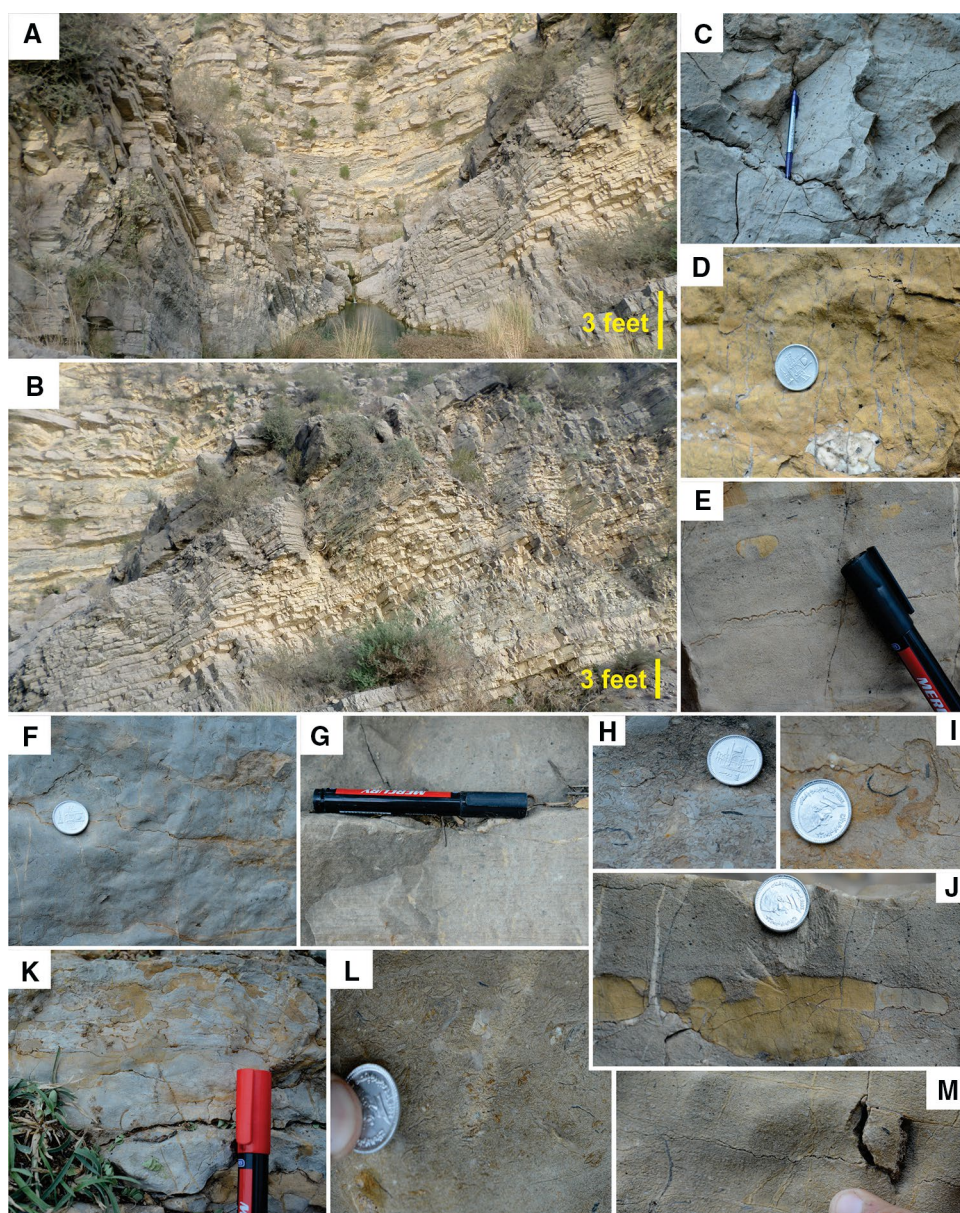


which bends eastward along a loop called Hazara Kashmir Syntax (Fig. 1). It emplaced Mesozoic strata over the Miocene on the northern periphery of Kohat and Potwar plateaus around 10 Ma [32, 37]. The MBT and associated structures in the subsurface may have played a crucial role in producing structural traps of hydrocarbon in both Kohat and Potwar Plateaus. Furthermore, the uplift along MBT has exposed the Samana Suk Formation for meteoric diagenesis and hence overprinted the diagenetic features within the unit.

The regional stratigraphy of the studied section ranges in age from Triassic to Miocene [19] (Fig. 1). The Triassic strata are comprised of a thick sequence of Kingriali Formation. The Early Jurassic is marked by regression, and the marine shelf is converted into a delta where diverse lithologies of the Datta Formation are deposited [38]. The

transgression during the Early Jurassic deposited a thick sequence of interbedded limestone and shale of Shinawari Formation [19, 39]. During Middle Jurassic, sea-level regressed and a thick sequence of shallow marine to marginal marine carbonates of the Samana Suk Formation is deposited [19]. In the study area, Samana Suk Formation is comprised of thin–medium–thick-bedded, micritic, bioclastic, and bioturbated limestone (Fig. 2a–c). The succession contains shale/marl horizons at different intervals (Fig. 2a, b). The rock unit includes calcite-filled fractures at different stratigraphic levels (Fig. 2d). Sedimentary structures/features including ripples, laminations, cross-beds, intraclasts, and siliciclasts are recorded at various stratigraphic horizons (Fig. 2e–h). The limestone of the Samana Suk Formation shows intense, small-scale, bedding parallel/perpendicular,

Fig. 2 Field photographs of Samana Suk Formation. **a, b** Thin- to thick-bedded limestone succession, **c** thick-bedded fractured, stylolitic micritic limestone. **d** Medium-bedded sandy limestone with calcite-filled fractures. **e** Coarse-grained, bioturbated, ripple marked limestone having small low-amplitude stylolites. **f** Medium-bedded, sandy, and bioturbated limestone. **g** Bedding parallel laminations in limestone. **h** Bioclast rich ripply, coarse-grained, thin-bedded limestone. **i** Coarse-grained, bioclastic, intraclastic, sandy, bioturbated limestone. **j, k** Stylolites engulf the bioturbated horizons in limestone. **l** Coarse-grained bioclastic, sandy, intraclastic, micritic limestone. **m** Bedding parallel stylolites and bedding perpendicular filled fractures in limestone



low-amplitude complex stylolites and fractures (Fig. 2i–k). At places, stylolites have stylo-nodular fabric (Fig. 2j, k). The uppermost part of the formation is an intraclastic, bioclastic sandy limestone (Fig. 2l, m). Based on palynology, vertebrate and invertebrate fossils, Bajocian to Early Oxfordian (160–170 Ma) age is given to the Samana Suk Formation [19]. The Samana Suk Formation is bounded by Late Jurassic to Early Cretaceous shelfal glauconitic sandstone and shale of the Chichali Formation and shoreface quartzose facies of the Lumshiwai Formation [19, 40]. The Upper Cretaceous strata are comprised of pelagic carbonates of the Kawagarh Formation, followed by Upper Paleocene carbonate platform sediments of Lockhart Formation and deep marine clays of Patala Formation [19]. The carbonate platform sediments of the Margalla Hill Limestone of Eocene overlie the Paleocene [41]. The Miocene molasse sediments of the Murree Formation represent the youngest sedimentary unit exposed in the study area [42].

3 Materials and Methods

A 380-foot-thick section of the Samana Suk Formation is measured and sampled in Sojhanda Section, Kala Chitta Range, Upper Indus Basin, Pakistan (Fig. 1). A total of 40 samples are collected at different intervals based on lithofacies variations within the succession. Thin sections preparation, petrography, scanning electron microscopic (SEM), and energy-dispersive X-ray spectroscopic (EDX) investigations are carried out at State Key Laboratory of Continental Dynamics, Northwest University, China. Representative photomicrographs are taken using Nikon Digital Sight DS-U3 camera fitted with the Polarizing Nikon Eclipse LV100N POL microscope. A total of 40 thin sections are used for defining the microfacies using the classification scheme of Dunham [43]. The constituents of carbonate rock including the type of grains, matrix, and cement are recorded. The semiquantitative data in percentages of the carbonate constituents are calculated using visual estimation charts of Baccelle and Bosellini [44]. For SEM analyses, centimeter-scale pieces of carbonate rocks are cut from each microfacies. The representative pieces are washed and dried using an electrical sample washer. The dried samples are gold-plated using BALTEC SCD 005 Coater. The detailed SEM analysis is carried out using FEI Quanta 450 Scanning Electron Microscopy equipped with a secondary electron detector (SE) and a backscatter electron detector (BSE). Representative samples are selected from microfacies for determining their high overburden pressure plug porosity, permeability, and production recovery rates. The samples are processed for making core plugs of 2.54 cm diameter. The analyses of high overburden pressure plug porosity,

permeability, and petroleum production recovery rates are carried out at Xi'an Shiyou University, China.

4 Results and Discussion

4.1 Microfacies Analysis

The microfacies are classified according to Dunham [43]. A total of eight microfacies are identified in the Samana Suk Formation. The established microfacies are compared with standard microfacies “SMF” types of Wilson [45] and Flügel [1]. The detailed description of the microfacies is given as below.

4.1.1 Mud Flat Microfacies

4.1.1.1 Mudstone Microfacies This microfacies is restricted to the upper uppermost part of the formation. It dominantly consists of lime mud matrix (95%), with allochems of bioclasts (3%) and rare siliciclastic quartz (Fig. 3a). Dissolution is seen under the SEM (Fig. 4a). The abundance of lime mud in microfacies indicates a calm water condition. The absence of biota hints toward hypersaline water [1]. This non-laminated, unfossiliferous, homogeneous micritic mudstone microfacies are indicative of low-energy supratidal environment, most probably mudflats or tidal ponds [46–48] (Fig. 6). The microfacies can be compared with SMF 23 Standard Microfacies (SMF) of Wilson [45] and Flügel [1].

4.1.1.2 Siliciclastic Dolo-Mudstone The siliciclastic dolo-mudstone microfacies is repeated at different stratigraphic heights in the section. The microscopic investigations delineate the dolomitized matrix (91%), siliciclastic quartz (5%), and peloids (4%) (Fig. 3b, c). Rare ooids and bioclasts are also observed (Fig. 3c). Calcite-filled fractures and low-amplitude stylolites are seen. The EDX and SEM analyses confirm the presence of fine-grained dolomite in the matrix which grades into ankerite at places (Fig. 4b, c). Intense dissolution on the grain margins of dolomite grains is also observed (Fig. 4c). The mudstone texture, dolomitized lime mud matrix, calcite-filled evaporative molds, and lack of marine biota, all suggest its deposition in low-energy hypersaline condition of mudflats [1, 47, 49] (Fig. 6). The microfacies is compared with SMF 23 Standard Microfacies (SMF) of Wilson [45] and Flügel [1]. Fine-grained siliciclasts are interpreted as windblown dust.

4.1.2 Lagoonal Microfacies

4.1.2.1 Peloidal Grainstone Peloidal grainstone microfacies is restricted to the middle part of the formation. It is comprised of peloids (51%), bioclasts (3%), gastropods

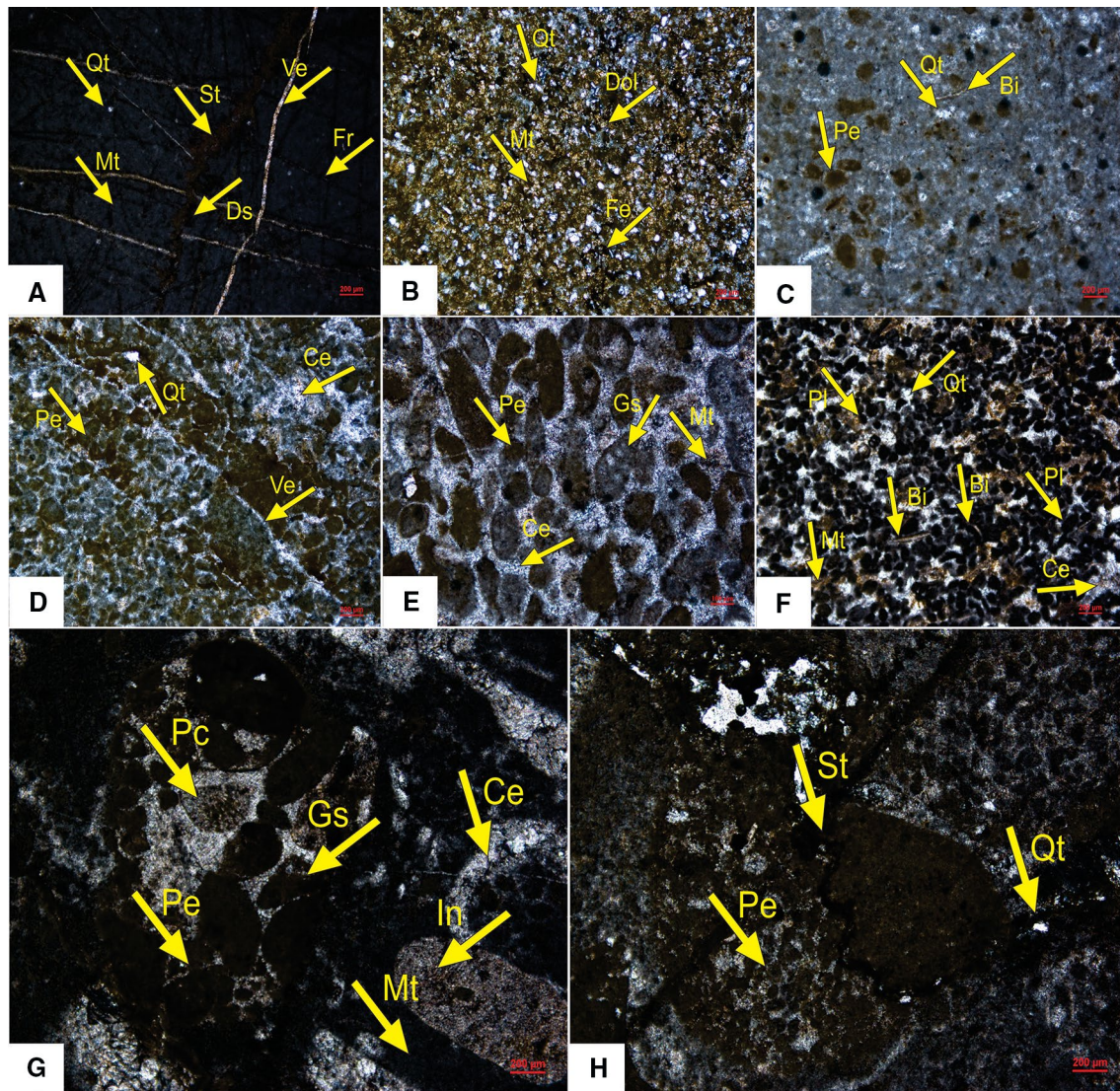


Fig. 3 Photomicrographs of various microfacies of Samana Suk Formation. **a** Mudstone. **b, c** Siliciclastic dolo-mudstone. **d, e** Peloidal grainstone. **f** Pelletal packstone. **g, h** Bioclastic peloidal wackestone.

Matrix (Mt), stylolites (St), vein (Ve), fracture (Fr), dissolution (Ds), quartz (Qt), bioclast (Bi), peloids (Pe), cement (Ce), pellets (Pl), iron (Fe), gastropods (Gs), pelecypod (Pc), intraclasts (In)

(2%), and ooids (1%) (Fig. 3d, e). The SEM images show dissolution (Fig. 4d). Rare siliciclasts are also observed (Fig. 3d). The allochems are cemented by spar (43%) (Fig. 3d, e). Elongated calcite-filled veins are seen throughout the microfacies. The EDX analyses reveal the presence of sparsely distributed organic matter (Fig. 4d). The grainstone texture and broken bioclasts indicate high-energy settings, while the presence of peloids indicates a low-energy setting [50]. The presence of gastropods show restricted lagoonal conditions [1, 49, 51]. It is therefore suggested that the microfacies is deposited in lagoonal tidal inlets with localized high-energy setting (Fig. 6). The peloids are either recycled from the middle shelf by storm surges or deposited in the calm water of the lagoon. The bioclasts indicate

a shallow environment with normal salinity and may have been transported to lagoonal tidal inlets during storm surges or tidal inlets. The microfacies correspond to SMF 16 of Wilson [45] and Flügel [1].

4.1.2.2 Pelletal Packstone The pelletal packstone microfacies is restricted to the middle–upper part of the formation. Based on the petrographic investigations, it is comprised of dark-colored pellets of uniform size (51%), bioclasts (5%), and micritic matrix (44%) (Fig. 3f). Moreover, microscopic calcite-filled fracture splays are also present (Fig. 3f). The dominant presence of mudstone texture indicates deposition in low-energy settings [1]. A large number of pellets in the micritic matrix suggest deposition on shallow subtidal to

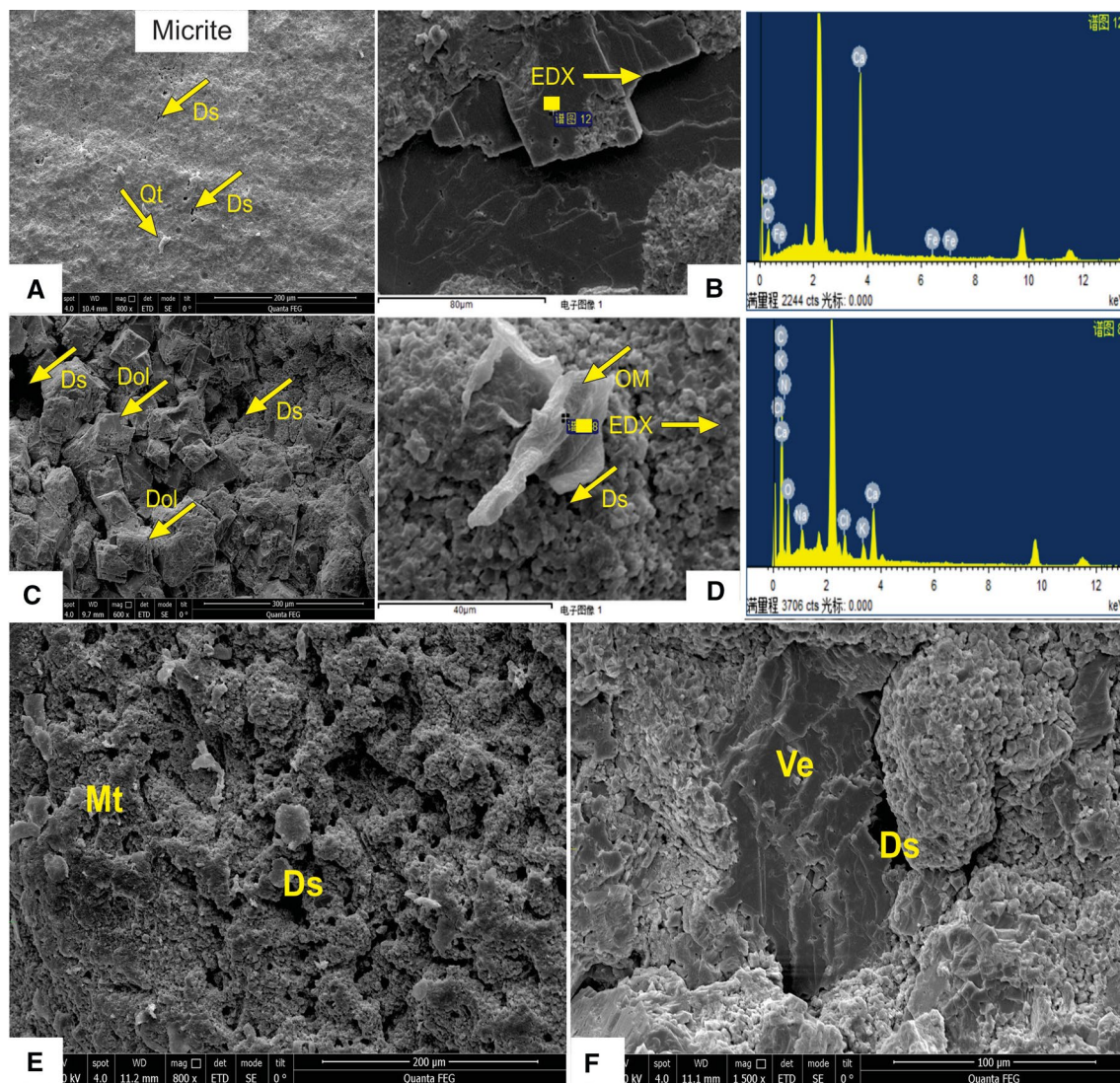


Fig. 4 SEM photomicrographs of various microfacies of Samana Suk Formation. **a** Mudstone. **b, c** Siliciclastic dolo-mudstone. **d** Peloidal grainstone. **e** Ooidal wackestone. **f** Intraclastic bioclastic peloidal

grainstone. Dissolution (Ds), quartz (Qt), dolomite (Dol), organic matter (OM), matrix (Mt), vein (Ve)

low-energy lagoonal environment [1, 47, 51] (Fig. 6). The microfacies correspond to the pelmicrite of SMF 22 Standard Microfacies (SMF) of Wilson [45] and Flügel [1].

4.1.2.3 Bioclastic Peloidal Wackestone The peloidal wackestone microfacies is recorded in the middle and upper part of the formation. Under the microscope, the microfacies is comprised of peloids (21%), bioclasts (7%), and intraclasts (1%) (Fig. 3g, h). Randomly distributed siliciclastic quartz grains (3%) are also observed (Fig. 3h). The microfacies is highly fractured and stylolitic (Fig. 3h). Stylolites show circular pattern constituting a nodular fabric. The abundant lime mud matrix with restricted fauna suggests that it is deposited in a lagoonal environment with a minor circulation [1, 49, 52] (Fig. 6).

4.1.3 Back Shoal Microfacies

4.1.3.1 Ooidal Wackestone The ooidal wackestone microfacies is restricted to the middle and uppermost part of the studied strata. The petrographic observations delineate ooids (14%), peloids (4%), echinoids (1%), and undifferentiated bioclasts (1%) (Fig. 5a–d). Rare dolomite crystals are also observed (Fig. 5c). Bedding parallel and perpendicular stylolites are present (Fig. 5d) along with fractures of various orientations. The SEM analyses reveal micro-vugs throughout the microfacies (Fig. 4e), while at places, intense dissolution is recorded (Fig. 4e). The ooids form in high-energy shoal settings of the inner shelf within the platform interior and restricted near-coast marginal marine settings [1, 53]. However, the high percentage of micritic matrix suggests

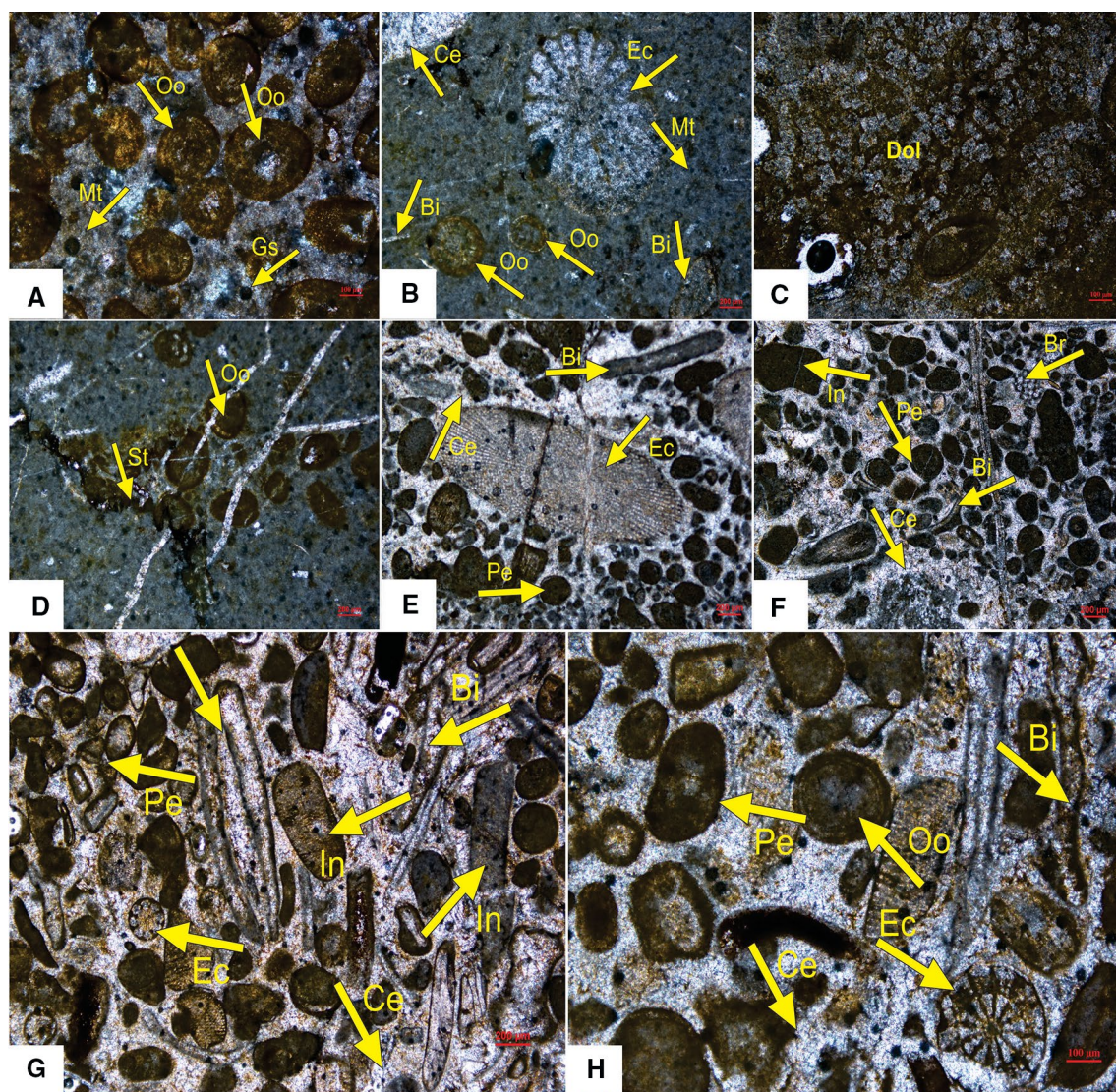


Fig. 5 Photomicrographs of various microfacies of Samana Suk Formation. **a–d** Ooidal wackestone. **e, f** Intraclastic bioclastic peloidal grainstone. **g, h** Ooidal peloidal bioclastic grainstone. Matrix (Mt),

ooid (Oo), gastropod (Gs), cement (Ce), echinoids (Ec), bioclast (Bi), dolomite (Dol), stylolites (St), peloids (Pe), intraclast (In), brachio-pods (Br)

calm water restricted conditions. The presence of restricted fauna like gastropod suggests a restricted lagoonal environment [1]. Ooids with ferruginous micritic envelopes, the abundance of micritic matrix, and restricted fauna suggest low-energy, restricted lagoonal conditions probably in back shoal [1, 47] (Fig. 6). The ooids are allochthonous in the lagoon. The microfacies can be correlated with SMF 15 M of Wilson [45] and Flügel [1].

4.1.4 Sand Shoal Microfacies

4.1.4.1 Intraclastic Bioclastic Peloidal Grainstone The intraclastic bioclastic peloidal grainstone microfacies is restricted to the middle part of the studied section. Based

on the petrography, it is composed of peloids (26%), undifferentiated bioclasts (17%), intraclasts (6%), gastropods (2%), echinoids (2%), miliolids (1%), brachiopods (1%), sponge spicules (1%), and ooids (1%) (Fig. 5e, f). Rare siliciclastic quartz grains are also observed. The peloids are partial to completely micritized (Fig. 5e, f). Some of the bioclasts show micritic rims, while others are completely micritized and are therefore indiscernible (Fig. 5e, f). The SEM analyses show calcite-filled vein and dissolution of the matrix (Fig. 4f). A large number of peloids are indicative of low-energy conditions. The bioclasts, pelecypods, brachiopods, and other skeletal fragments hint toward the shallow marine environment with normal salinity. The presence of intraclasts, bioclasts, and ooids indicates high-energy con-

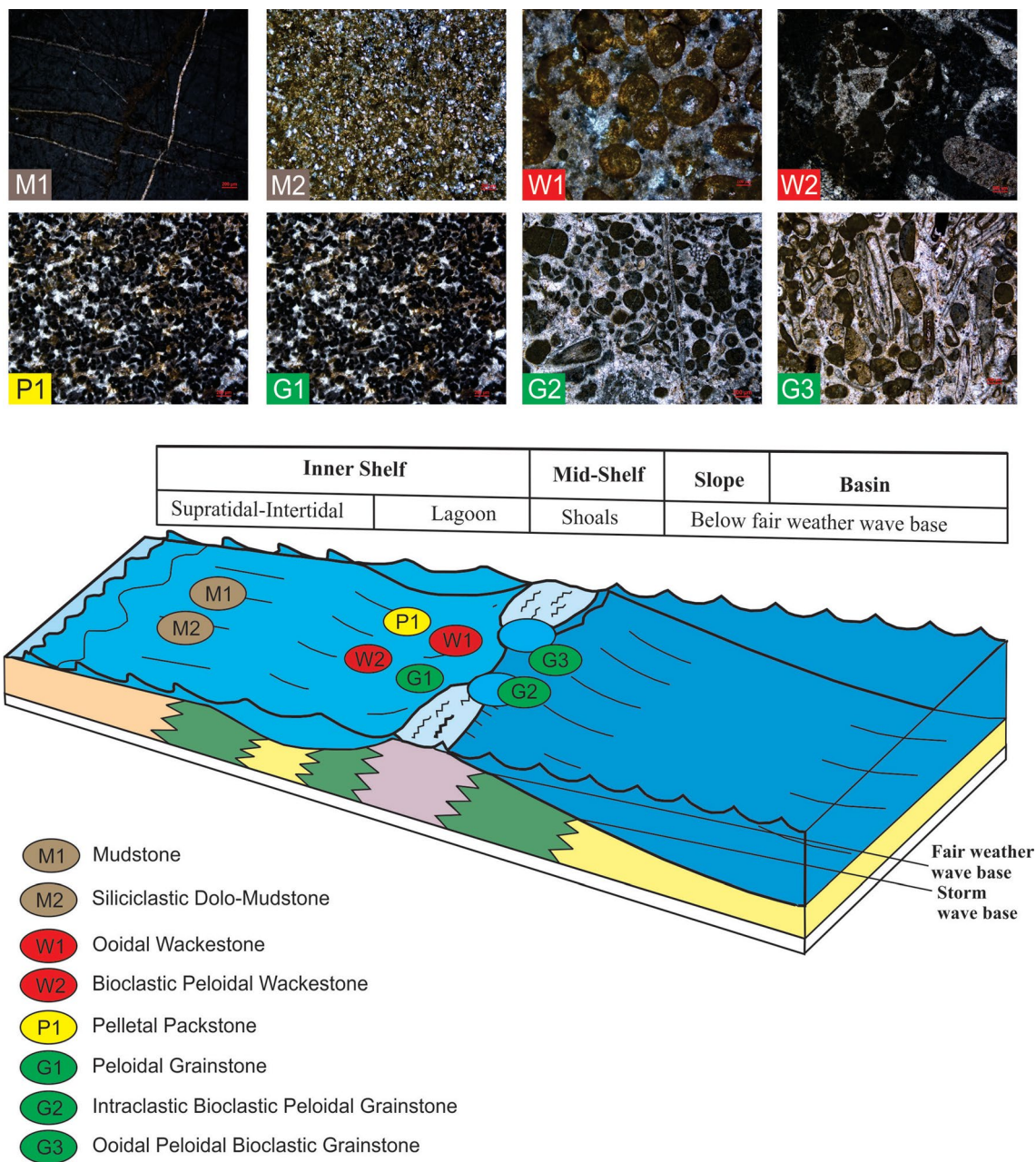


Fig. 6 Depositional model showing the interpreted depositional environments of Samana Suk Formation in the Kala Chitta Range

ditions above Fair Weather Wave Base [1, 49]. Based on these shreds of evidence, it is suggested that the microfacies is deposited in the nearshore zone of the inner shelf environment inundated by occasional storms (Fig. 6). The peloids of low-energy conditions are reworked into such high-energy settings.

4.1.4.2 Ooidal–Peloidal Bioclastic Grainstone The ooidal–peloidal bioclastic grainstone microfacies is located within the middle part of the studied section. It is comprised of bioclasts (35%), brachiopods (1%), cephalopods (2%), mili-

olids (1%), echinoids (2%), gastropods (2%), peloids (7%), ooids (5%), and intraclasts (1%) (Fig. 5g, h). Most of the bioclasts are completely micritized and coated. At places, the recrystallization of bioclasts is observed. Selective micritization and micritic envelope have been observed. Ooidal grapestone is also seen. The micritized ooids and ooidal grapestone form as a result of biogenic encrustations in protected lagoonal settings [1]. The presence of peloids, miliolids, and gastropods also suggests lagoonal settings [1]. Bioclast, pelecypods, brachiopods, and other skeletal fragments hint toward a shallow marine environment with

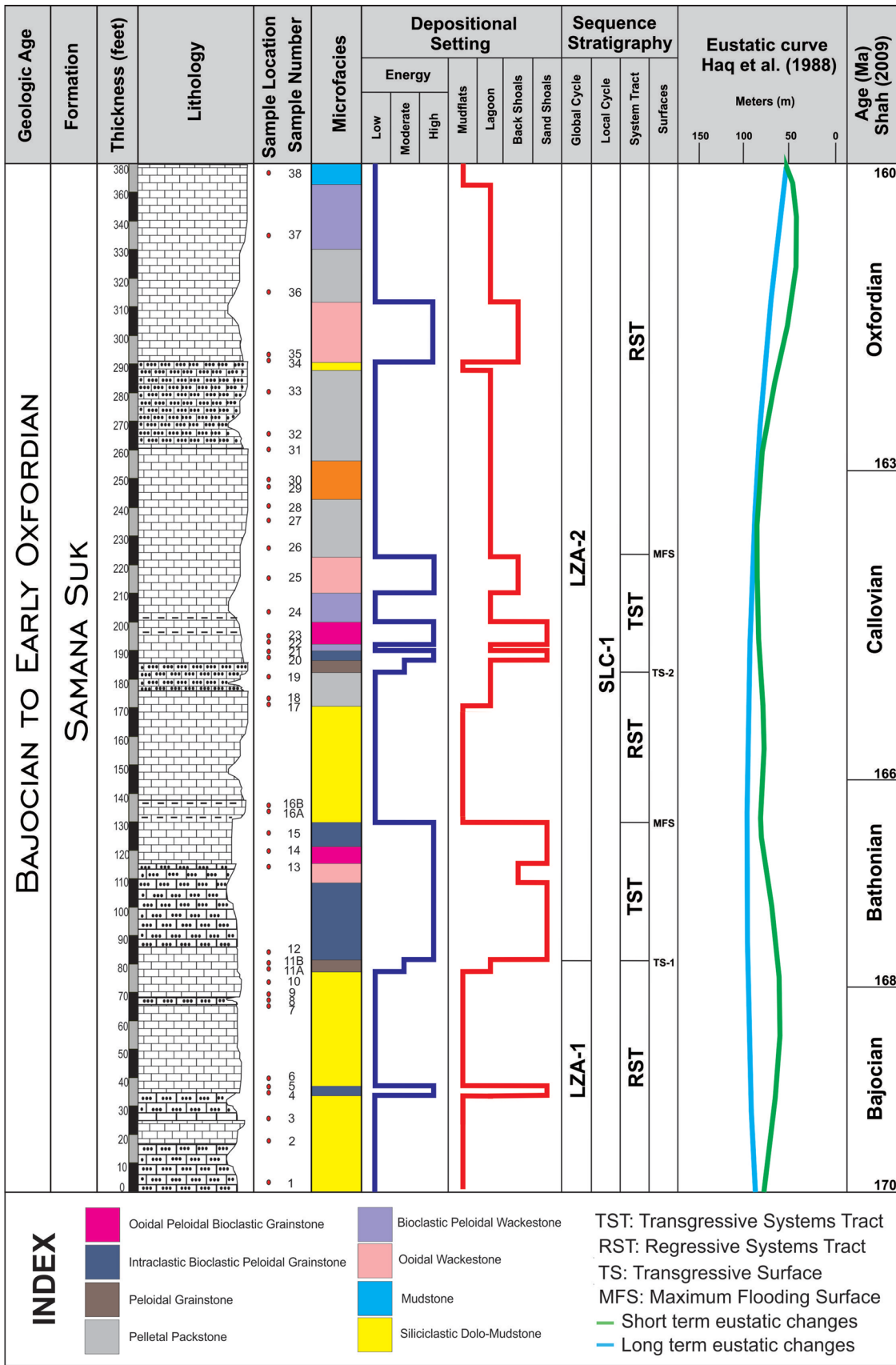


Fig. 7 Stratigraphic log showing varying lithology, distribution of microfacies types, depositional setting, sequence stratigraphy, and eustatic curve of the Samana Suk Formation

normal salinity. The ooids form in high-energy shoal settings of the inner shelf within the platform interior, which is restricted to near-coast marginal marine settings [1, 53] (Fig. 6). The high-energy condition is further supported by the dominance of sparite. Initially, the ooids are reworked to the low-energy restricted lagoon and are deposited in association with miliolids and gastropods. The ooids are encrusted and micritized forming grapestone fabric. Later on, the ooids and intraclasts are reworked to high-energy inner shelf and deposited in normal marine conditions above Fair Wave Base (FWWB). This microfacies corresponds to SMF 11 of Wilson [45] and Flügel [1].

4.2 Depositional Model

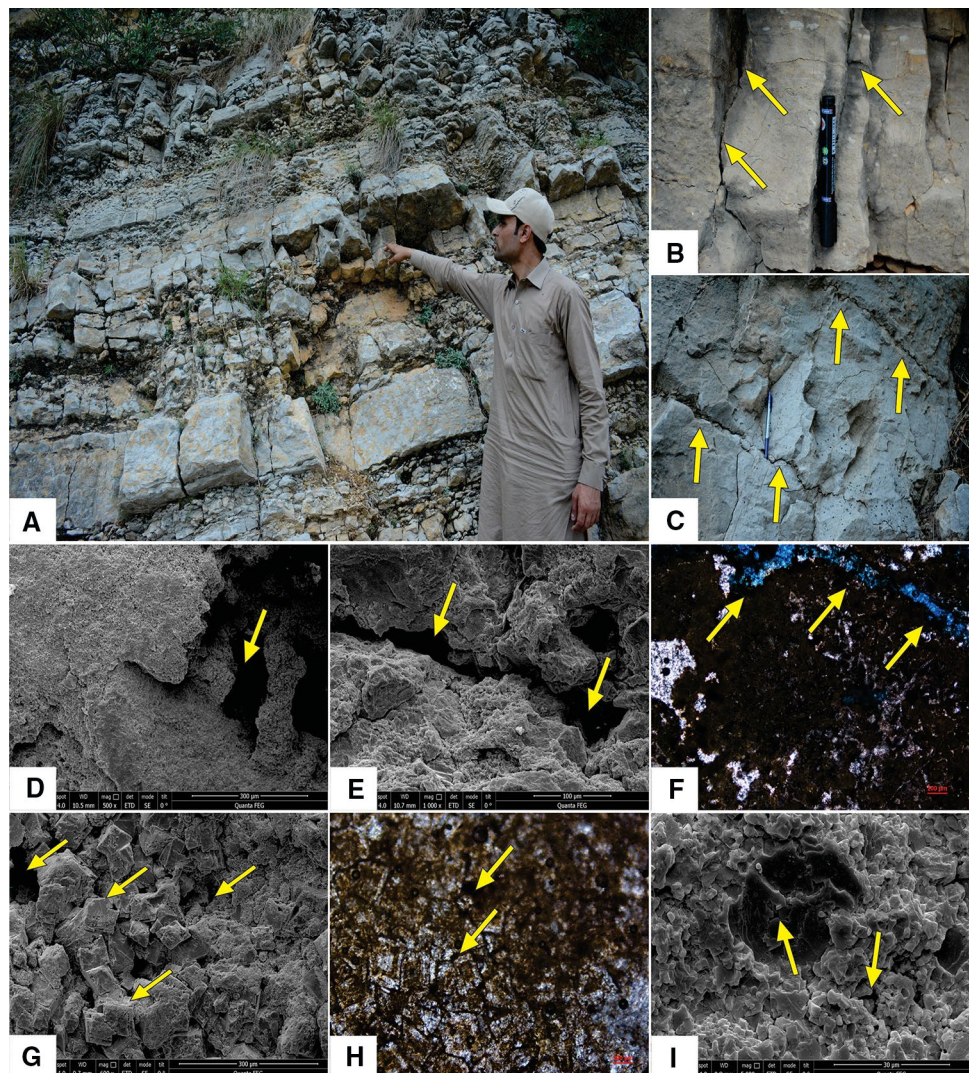
The lower part of the Samana Suk Formation is deposited in the mudflats environment (Figs. 6, 7). This interpretation is based on the dominance of mudstone microfacies. The lower part grades into grainstone microfacies in its upper

portion, which is deposited in sand shoals. The middle part is dominantly deposited in the lagoonal environment with some back shoal facies (Figs. 6, 7). The lagoonal interpretation is supported by the presence of allochthonous ooids, bioclasts, and restricted/reworked fauna in mudstone, wackestone, packstone textures. The upper part is deposited in mudflat settings with minor back shoal facies (Figs. 6, 7). The Samana Suk Formation in the studied stratigraphic section is deposited mainly in the mudflat and lagoonal settings, with some parts in the sand shoal and back shoal settings. Most Middle Jurassic carbonates elsewhere in the world are also mainly deposited in similar depositional environments.

4.3 Sequence Stratigraphic Modeling

Sequence stratigraphy deals with facies relationships and stratal architecture within a chronostratigraphic framework [54, 55]. It focuses on the subdivision of strata into genetically related units, i.e., sequence, systems tracts,

Fig. 8 Photographs showing various types of porosity. **a** Interbedded fractured limestone and shales. **b, c** Fractured limestone. **d, e** SEM photographs showing intense dissolution. **f** Dissolution cavities in various microfacies. **g** SEM photograph showing porosity associated with dolomites. **h** Dolomitization and associated micro-pores, **i** Intra-particle and inter-particle porosity



parasequences which are resulted from the interplay of accommodation and sedimentation [55]. Although the division of the homogenous carbonate lithologies into a distinct genetic unit is quite challenging [56, 57], the in situ nature of carbonate sediments makes them susceptible to changes in the environment. The changes in water depth control a wide range of environmental conditions, e.g., light penetration, oxygenation, energy, temperature, nutrients, CO₂ balance, salinity, and siliciclastic input [58]. All these factors control the growth of carbonate sediments; therefore, a slight sea-level change will cause a drastic change in the type of carbonate sediments. The microfacies analyses can be used efficiently for establishing a change in depositional environments as a result of the change in relative sea level. However, distinctive temporal changes in microfacies of the studied section are used for defining the sea-level changes.

The relative sea-level curve for Samana Suk Formation is constructed from the microfacies data (Fig. 7). The 10 Ma (170–160 Ma) depositional time of the Samana Suk Formation is divided into equal time slices throughout the stratigraphic section. Thus, the depositional cycles are put into a chronostratigraphic framework. The sequence stratigraphy of the unit is established using Embry and Johannessen model [59]. Based on the chronostratigraphic framework, the Samana Suk Formation is deposited in one second-order local cycle (SLC-1). The cycle correlates with fine-tuned global LZA-1 and LZA-2 sequences of Haq et al. [60] (Fig. 7). In SLC-1, three regressive systems tracts (RSTs) and two transgressive systems tracts (TSTs) have been recorded within the Samana Suk Formation (Fig. 7). The carbonate systems tracts are usually composed of deepening upward units bounded by flooding surface [61, 62].

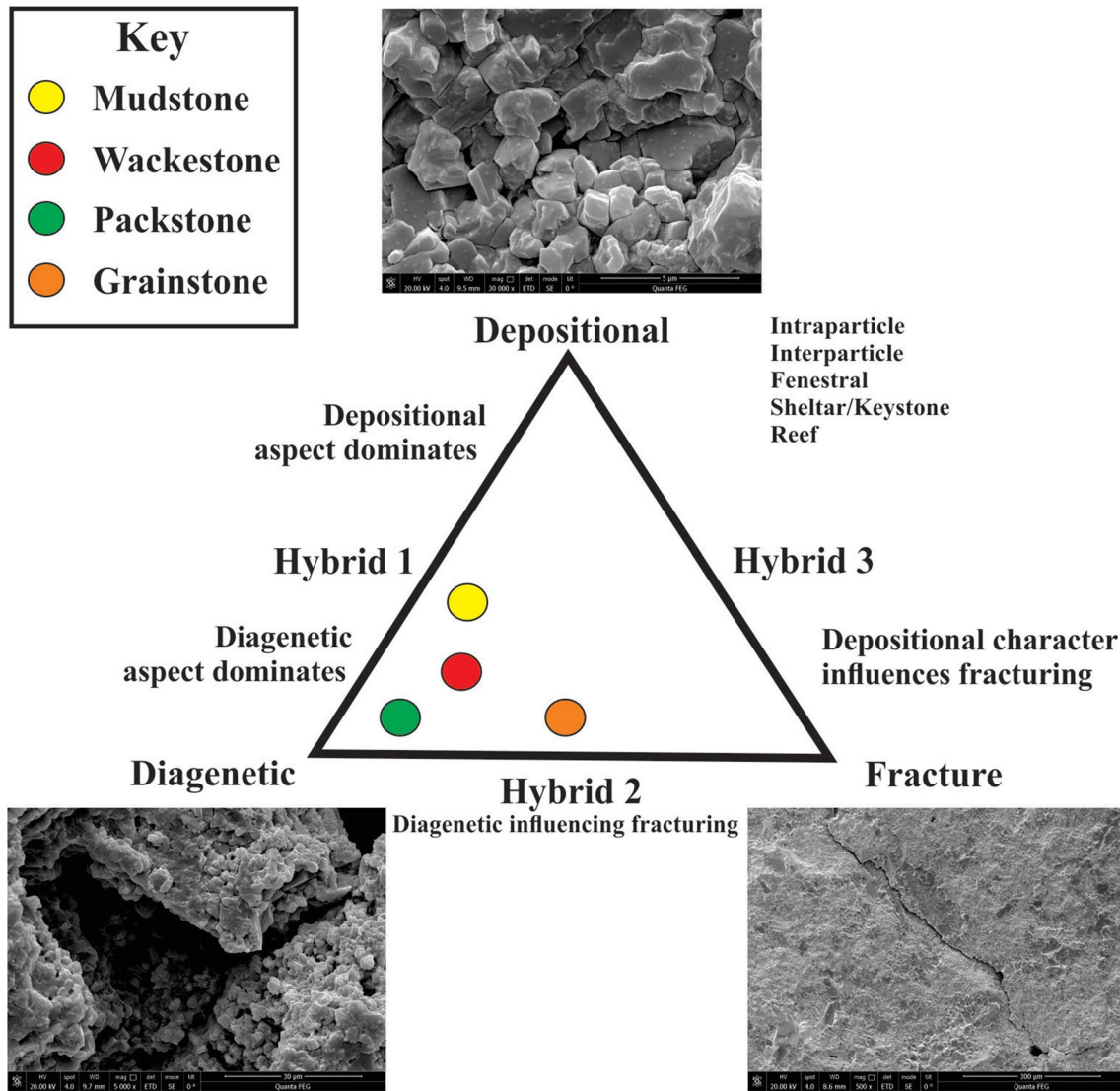


Fig. 9 Genetic classification of porosity for the Samana Suk Formation (modified after Ahr [68])

However, a high-resolution study is required to identify these small-scale parasequences.

4.3.1 Systems Tracts

The lowermost part of Samana Suk Formation is characterized by siliciclastic mudstone microfacies of lagoon and mudflats (Fig. 7) indicating sea-level low stand of RST-1 (Fig. 7). The progradation has established shallow marine to marginal marine carbonate sedimentation (Bajocian-Oxfordian) over the underlying deeper carbonates/shale sequence of Toarcian Shinawari Formation [19]. The lagoonal mud flat carbonates of RST-1 are overlain by intraclastic–bioclastic–peloidal grainstone and ooidal–peloidal–bioclastic

grainstone microfacies of carbonate sand shoal which indicate retrogradation of carbonate platform (Fig. 7). This landward shift in facies migration is marked as TST-1. Based on the alternating repetitions of lagoon/mudflats facies (siliciclastic mudstone, mudstone, ooidal wackestone, pelletal packstone) with carbonate sand shoals facies (intraclastic–bioclastic–peloidal grainstone, peloidal grainstone, and ooidal–peloidal–bioclastic grainstone microfacies), RST-2, TST-2, and RST-3 are defined (Fig. 7). The RST's carbonate packages are thicker as compared to those of the TST's due to their higher sedimentation rates during the phase of sea-level low stands (Fig. 7).

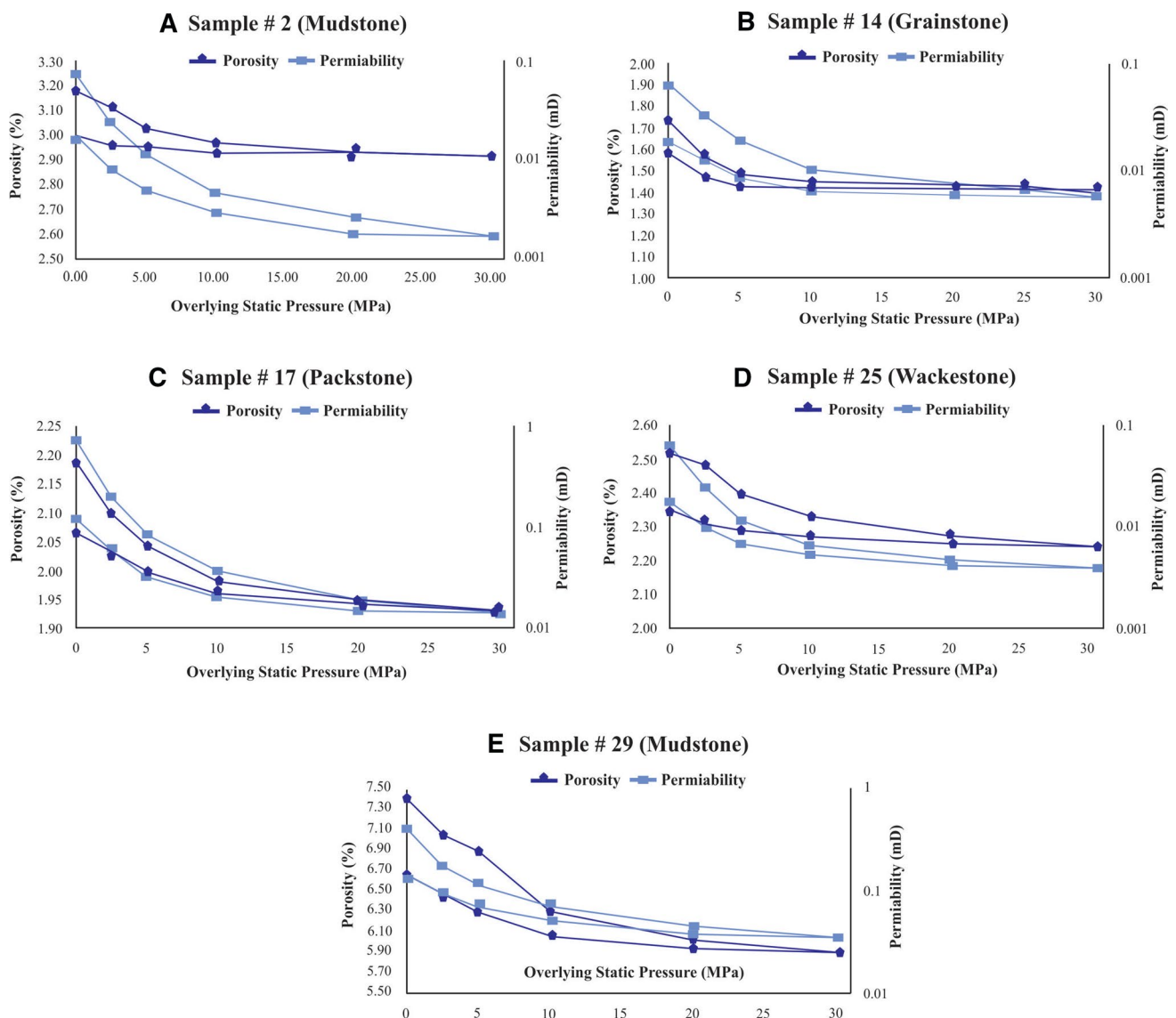


Fig. 10 Relationship between porosity and permeability of selected samples (sample # 2, 14, 17, 25, and 29) from mudstone, wackestone, packstone, and grainstone microfacies at various overlying static pressures

4.3.2 Correlation with Global Events

The relative sea-level curve constructed for the Samana Suk Formation is plotted against the global sea-level curve (Fig. 7) in 170–160 Ma time interval. The correlation shows a perfect match with a long-term global sea-level fall (Fig. 7) [60]. However, when compared with individual Jurassic events, the correlation of the studied section shows quasi-correlation. For example, the studied section shows a relative sea-level fall during Bajocian (Fig. 7), while the same interval is recognized as a global transgressive event [63]. Regionally, this transgressive event is documented in southern France, northern Switzerland, and southern Andes [64, 65]. Similarly, the Late Bajocian is also documented as a transgressive event in different parts of the world (e.g., northern Europe, Greenland, and Argentina) [64–66]. The correlation of the studied section with other parts of the world [64–66] shows that the RST-1 of the studied section is deposited during Bajocian in relative sea-level fall as compared to global sea-level rise (Fig. 7). Furthermore, the studied section shows a relative sea-level rise during Bathonian while it is considered as an anomalous eustatic sea-level fall (i.e., showing regional pulses in sea-level rise) (Fig. 7) [63, 67]. Therefore, the TST-1 in the studied section might represent the regional expression (relative sea-level rise) of the Bathonian event. The lower part of RST-2 is also deposited

within this event. The studied section has preserved phases of both sea-level fall and rise during the Callovian (Fig. 7). The Late Callovian is recorded as a eustatic sea-level rise, while the Early Callovian is considered as a eustatic sea-level rise of diachronous nature [63]. The RST-2 of the studied section may represent a regional regressive expression of the Early Callovian event, while the TST-2 correlates well with the Late Callovian eustatic sea-level rise (Fig. 7). Furthermore, in the study area, the Early Oxfordian is preserved as a regressive episode while it is considered as an event of global transgression and condensation (Fig. 7) [63, 64]. Therefore, the deposition of RST-3 does not correlate with its global counterparts. It is evident that although the relative sea level of the Samana Suk Formation correlates with long-term global sea level, the depositional cycles of the succession indicate quasi-correlation with global events (Fig. 7). Therefore, the genetic units within the Samana Suk Formation are only partially controlled by global events.

4.4 Porosity and Permeability Analyses

The outcrop observation reveals that the limestone of the Samana Suk Formation is highly fractured (Fig. 8a–c). Such interconnected fractures have offered secondary porosity and permeability to the Samana Suk Formation and may have enhanced the reservoir potential of the unit.

Table 1 Overburden high-pressure plug porosity and permeability results of the selected rock samples (sample # 2, 14, 17, 25, and 29) from mudstone, wackestone, packstone, and grainstone microfacies of the Middle Jurassic Samana Suk Formation

Sample # 02 (mudstone)													
Pressure (MPa)	0	2.51	5.02	10.1	20.2	30.2	20.0	10.1	5.11	2.60	0.01	Recovery rate (%)	
Porosity (%)	3.18	3.11	3.03	2.97	2.93	2.92	2.92	2.93	2.95	2.96	2.99	Porosity	Permeability
Permeability (mD)	0.074	0.023	0.011	0.004	0.002	0.001	0.001	0.002	0.004	0.007	0.014	94.03	20.17
Sample # 14 (grainstone)													
Pressure (MPa)	0.00	2.48	5.01	10.0	25.1	30.0	20.0	10.0	5.02	2.51	0.02	Recovery rate (%)	
Porosity (%)	1.73	1.58	1.50	1.45	1.42	1.40	1.41	1.42	1.43	1.47	1.58	Porosity	Permeability
Permeability (mD)	0.063	0.033	0.019	0.010	0.006	0.005	0.005	0.006	0.008	0.012	0.018	91.33	29.35
Sample # 17 (packstone)													
Pressure (MPa)	0.00	2.50	5.03	10.0	20.2	30.0	20.0	9.97	5.02	2.51	0.03	Recovery rate (%)	
Porosity (%)	2.19	2.10	2.04	1.98	1.95	1.94	1.95	1.97	2.00	2.03	2.06	Porosity	Permeability
Permeability (mD)	0.716	0.202	0.082	0.037	0.019	0.014	0.015	0.020	0.032	0.059	0.125	94.28	17.44
Sample # 25 (wackestone)													
Pressure (MPa)	0.00	2.55	5.01	10.0	20.0	30.5	20.2	10.1	5.02	2.51	0.02	Recovery rate (%)	
Porosity (%)	2.52	2.48	2.40	2.33	2.27	2.24	2.25	2.27	2.29	2.32	2.35	Porosity	Permeability
Permeability (mD)	0.063	0.024	0.011	0.006	0.005	0.004	0.004	0.005	0.006	0.009	0.018	93.29	28.69
Sample # 29 (mudstone)													
Pressure (MPa)	0.00	2.52	5.03	10.0	20.1	30.2	20.1	10.2	5.02	2.52	0.03	Recovery rate (%)	
Porosity (%)	7.40	7.05	6.88	6.32	6.04	5.90	5.93	6.05	6.30	6.46	6.66	Porosity	Permeability
Permeability (mD)	0.404	0.173	0.113	0.068	0.045	0.035	0.039	0.051	0.072	0.093	0.140	89.95	34.64

The petrographic and SEM studies show dissolution with micro-vugs and molds in mudstone and wackestone microfacies having high interconnectivity (Fig. 8d–f). The distribution of organic matter within the mudstone and wackestone microfacies and associated dissolution of the micritic matrix suggested that dissolution has resulted from methane exhalation during the decay of algal organic matter [1]. Furthermore, the lack of early diagenetic dissolution in grainstone is assigned to the continuous replenishment of oxygenated water in the pores, which has inhibited the preservation of organic matter. The petrographic and SEM observations reveal intense dolomitization in mudstone and wackestone microfacies (Fig. 8g, h). The SEM studies show uniform distribution of micropores formed during the dolomitization with fair interconnectivity (Fig. 8g), which contribute both porosity and permeability in the studied section. The SEM observations also show inter-particle and intra-particle porosity in mudstone and wackestone microfacies (Fig. 8i). Porosity types observed in the rock unit are the outcome of depositional, diagenetic, and fracturing processes. Considering these processes, we classified the porosity according to the triangular diagram of Ahr [68] (Fig. 9). Based on the diagram, most of the microfacies have dissolution porosity which is supplemented by depositional and fracture porosity. No pronounced porosity is observed in grainstone microfacies probably because the primary inter-granular pore spaces are plugged by heavy cementation.

The high overburden pressure plug porosity and permeability analyses of each microfacies made at eleven different pressures show higher porosity and permeability in the mudstone and wackestone microfacies than those in the grainstone (Fig. 10; Table 1). The results also show decreasing porosity and permeability with increasing burial pressures (Fig. 10; Table 1). The cross-plots show that porosity and permeability decrease uniformly with depth in almost all microfacies except the dolo-mudstone, whereby the permeability decrease is drastic in relation to a decrease in porosity. The data of production recovery rates measured in percentages on selected microfacies show high values of recovered porosity and permeability (Fig. 10; Table 1). This, in turn, suggests a strong interconnectivity of pores in all the microfacies.

5 Summary and Conclusions

The Middle Jurassic shallow to marginal marine carbonates is deposited in different stratigraphic sections of the world including Turkey, Oman, southern Tibet, southern Montenegro, Iberian Peninsula, Italy, France, and Morocco [69–76]. Furthermore, the Jurassic carbonates are major hydrocarbon reservoirs in the Middle East and its surrounding [77–80]. Similar shallow marine carbonates

of the Samana Suk Formation are widely deposited in the Indus Basin, Pakistan [19]. The shallow to marginal marine carbonates of the Samana Suk Formation is a good analog of similar carbonates of the world due to its widespread distribution, lithological, petrographic, and diagenetic variations. Therefore, the formation is selected as an example to evaluate the role of sequence stratigraphy in the reservoir potential of Middle Jurassic shallow to marginal marine carbonates. The petrographic and SEM studies reveal eight microfacies deposited in different depositional settings including mudflats, lagoon, back shoals, and sand shoals. The carbonates of Samana Suk Formation have recorded one second-order cycle (SLC1), two TSTs, and three RSTs. The porosity and permeability of the Samana Suk Formation are investigated using field, petrographic, SEM, EDX, and high overburden pressure plug porosity and permeability analyses. On outcrop, the Samana Suk Formation shows wide and elongated interconnected fractures throughout the succession. In addition, low- to high-amplitude interconnected stylolites are also observed. The interconnected fractures and stylolites may have significantly enhanced the porosity and permeability of the Samana Suk Formation. Although the concentration of insoluble residue along stylolites may hinder the fluid flow, such insoluble seams are almost absent at the outcrop level. The petrographic, SEM, EDX, high overburden pressure plug porosity and permeability analyses of the Samana Suk Formation reveal significantly high porosity and permeability within all mudstones and wackestone microfacies deposited in RST than grainstones of TST. The dominant porosity types observed in these microfacies are inter-crystalline and syn-sedimentary dissolution. The rare porosity observed in grainstone microfacies deposited in high-energy shoal settings of TST has resulted from the heavy cementation which is likely associated with dissolution during the telogenetic stage of diagenesis. The higher rates of production recoveries for all microfacies suggest high interconnectivity of pores.

The multitude of depositional and diagenetic processes has produced higher porosity and permeability in the mudstone to wackestone microfacies of RST and therefore carries relatively high reservoir potential. Conversely, the heavy cementation and lack of early diagenetic dissolution in grainstone microfacies of the TST have caused lower porosity and permeability, hence lower reservoir potential. However, widespread large fractures, dissolution cavities, vugs, and stylolites at the outcrop scale have been added significantly to the overall reservoir potential of the Samana Suk Formation, hence a good reservoir.

Acknowledgements The authors are thankful to the State Key Laboratory of Continental Dynamics, Northwest University, China, for providing facilities to carry out laboratory analysis. Authors are also thankful

to the Department of Geology, University of Swabi and Department of Geology, University of Peshawar, Pakistan, for support and help. Thanks are extended to Mr. Hikmat Salam, Mr. Ali Rahman, Mr. Zhang Dongdong, Mr. Yang Kang, Mr. Zhang Weijie, and Ms. Peng Yifeng for their help and support during the field and laboratory work.

Funding Not applicable.

Code Availability Not applicable

Compliance with Ethical Standards

Conflict of interest The authors declare that they have no conflict of interest.

Availability of Data and Materials Not applicable.

References

- Flügel, E.: *Microfacies of Carbonate Rocks: Analysis, Interpretation*, vol. 1, pp. 1–996. Berlin and Heidelberg GmbH & Co., Berlin (2004)
- Morad, S.; Ketzer, J.; De Ros, L.F.: Spatial and temporal distribution of diagenetic alterations in siliciclastic rocks: implications for mass transfer in sedimentary basins. *Sedimentology* **47**, 95–120 (2000)
- Read, J.; Horbury, A.D.: Eustatic and tectonic controls on porosity evolution beneath sequence-bounding unconformities and parasequence disconformities on carbonate Platforms. In: Horbury, A., Robinson, A.G. (eds.) *Diagenesis and Basin Development*, pp. 155–197. AAPG, Tulsa (1993)
- Tucker, M.E.: Carbonate diagenesis and sequence stratigraphy. In: Wright, P.V. (ed.) *Sedimentology Review/1*, pp. 51–72. Blackwell Scientific Publications, Oxford (1993)
- Morad, S.; Ketzer, J.; DeRos, L.: Linking diagenesis to sequence stratigraphy: an integrated tool for understanding and predicting reservoir quality distribution. *Link. Diag. Seq. Stratigr. Spec. Publ. Int. Assoc. Sedimentol.* **45**, 1–36 (2012)
- Hart, B.; Longstaffe, F.; Plint, A.: Evidence for relative sea level change from isotopic and elemental composition of siderite in the Cardium Formation, Rocky Mountain Foothills. *Bull. Can. Pet. Geol.* **40**(1), 52–59 (1992)
- Morad, S.: Carbonate cementation in sandstones: distribution patterns and geochemical evolution (Ed. S. Morad), *Carbonate Cementation in Sandstones. Int. Assoc. Sedimentol. Spec. Publ.* **26**, 1–26 (1998)
- Morad, S.; Al-Ramadan, K.; Ketzer, J.M.; De Ros, L.: The impact of diagenesis on the heterogeneity of sandstone reservoirs: a review of the role of depositional facies and sequence stratigraphy. *AAPG Bull.* **94**(8), 1267–1309 (2010)
- Cross, T.A.: Controls on Coal Distribution in Transgressive-Regressive Cycles. *Upper Cretaceous, Western Interior* (1988)
- Whalen, M.T.; Eberli, G.P.; Van Buchem, F.S.; Mountjoy, E.W.; Homewood, P.W.: Bypass margins, basin-restricted wedges, and platform-to-basin correlation, Upper Devonian, Canadian Rocky Mountains: implications for sequence stratigraphy of carbonate platform systems. *J. Sediment. Res.* **70**(4), 913–936 (2000)
- Posamentier, H.W.; Allen, G.P.: *Siliciclastic Sequence Stratigraphy: Concepts and Applications*, vol. 7. SEPM (Society for Sedimentary Geology) Tulsa, Oklahoma (1999)
- Tucker, M.E.; Wright, V.P.: *Carbonate Sedimentology*. Wiley, Berlin (2009)
- Middlemiss, C.S.: *The Geology of Hazara and the Black Mountain*. Geological Survey, Peshawar (1896)
- Latif, M.: Explanatory notes on the geology of southeastern Hazara to accompany the revised geological map. *Jahrbuch der Geologischen Bundesanstalt Sonderband* **15**, 5–20 (1970)
- Cotter, G.D.P.: The geology of the part of the Attock district west of longitude 72 45 E. *Mem. Geol. Surv. India* **55**(2), 63–161 (1933)
- Gee, E.R.: Further Note on the Age of the Saline Series of the Punjab and of Kohat. Pioneer Press, New York (1947)
- Calkins, J.A.; Matin, A.A.: The geology and mineral resources of the Garhi Habibullah quadrangle and the Kakul area, Hazara District, Pakistan. *United States Geological Survey*, pp 2331–1258 (1973)
- Davis, W.M.: Origin of limestone caverns. *Bull. Geol. Soc. Am.* **41**(3), 475–628 (1930)
- Shah, S.M.I.: Stratigraphy of Pakistan. *Geol. Surv. Pak. Mem.* **22**, 265 (2009)
- Qureshi, M.K.A.; Butt, A.A.; Ghazi, S.: Shallow shelf sedimentation of the Jurassic Samana Suk Limestone, Kala Chitta Range, Lesser Himalayas, Pakistan. *Geol. Bull. Punjab Univ.* **43**, 1–14 (2008)
- Nizami, A.R.; Sheikh, R.A.: Microfacies analysis and diagenetic study of Samana Suk Formation, Chichali Nala Section, Surghar Range. *Trans Indus Ranges, Pakistan. Geol. Bull. Punjab Univ.* **42**, 37–52 (2007)
- Mertmann, D.; Ahmad, S.: Shinawari and Samana Suk Formations of the Surghar and Salt Ranges, Pakistan: facies and depositional environments. *Zeitschrift der Deutschen Geologischen Gesellschaft* **30**, 5–17 (1994)
- Bender, F.K.; Raza, H.A.: *Geology of Pakistan. Beiträge zur regionalen Geologie der Erde. Gebrüder Borntraeger Berlin* **25** (1995)
- Fatmi, A.; Hyderi, I.; Anwar, M.: Occurrence of the Lower Jurassic Ammonoid Genus *Bouleiceras* from the Surghar Range with a Revised Nomenclature of the Mesozoic Rocks of the Salt Range and Trans Indus Ranges (Upper Indus Basin). *Geol. Bull. Punjab Univ.* **25**, 38–46 (1990)
- Hallam, A.; Maynard, J.: The iron ores and associated sediments of the Chichali formation (Oxfordian to Valanginian) of the Trans-Indus Salt Range, Pakistan. *J. Geol. Soc.* **144**(1), 107–114 (1987)
- Hussain, H.S.; Fayaz, M.; Haneef, M.; Hanif, M.; Jan, I.U.; Gul, B.: Microfacies and diagenetic-fabric of the Samana Suk Formation at Harnoi Section, Abbottabad, Khyber Pakhtunkhwa, Pakistan. *J. Himal. Earth Sci.* **46**(2), 41–53 (2013)
- Ali, F.; Haneef, M.; Anjum, M.N.; Hanif, M.; Khan, S.: Microfacies analysis and sequence stratigraphic modeling of the Samana Suk Formation, Chichali Nala, Trans Indus Ranges, Punjab, Pakistan. *J. Himal. Earth Sci.* **46**(1), 41–53 (2013)
- Hayat, M.; ur Rahman, M.; Khan, N.A.; Ali, F.: Sedimentology, Sequence Stratigraphy and Reservoir Characterization of Samana Suk Formation Exposed in Namal Gorge Section, Salt Range, Mianwali, Punjab, Pakistan. *Int. J. Econ. Environ. Geol.* **7**(1), 4–15 (2016)
- Shah, M.M.; Ahmed, W.; Ahsan, N.; Lisa, M.: Fault-controlled, bedding-parallel dolomite in the middle Jurassic Samana Suk Formation in Margalla Hill Ranges, Khanpur area (North Pakistan): petrography, geochemistry, and petrophysical characteristics. *Arab. J. Geosci.* **9**(5), 405 (2016)
- Rowley, D.B.: Age of initiation of collision between India and Asia: a review of stratigraphic data. *Earth Planet. Sci. Lett.* **145**(1–4), 1–13 (1996)



31. Coward, M.P.; Butler, R.; Chambers, A.; Graham, R.; Izatt, C.; Khan, M.A.; Knipe, R.J.; Prior, D.; Treloar, P.J.; Williams, M.: Folding and imbrication of the Indian crust during Himalayan collision. *Philos. Trans. R. Soc. Lond. Ser. A Math. Phys. Sci.* **326**(1589), 89–116 (1988)
32. Yeats, R.S.; Hussain, A.: Timing of structural events in the Himalayan foothills of northwestern Pakistan. *Geol. Soc. Am. Bull.* **99**(2), 161–176 (1987)
33. Calkins, A.J.; Offield, W.T.; Abdullah, S.K.M.; Ali, S.T.: Geology of the southern Himalaya in Hazara, Pakistan and adjacent areas. In: US Geological Survey Professional Paper 716-C, pp. 29. Denver, Colorado (1975)
34. Powell, C.M.: A speculative tectonic history of Pakistan and surroundings. *Geodynamics of Pakistan* (1979)
35. Kadri, I.B.: *Petroleum Geology of Pakistan*. Pakistan Petroleum Limited (1995)
36. DiPietro, J.A.; Pogue, K.R.: Tectonostratigraphic subdivisions of the Himalaya: a view from the west. *Tectonics* **23**(5), 510–525 (2004)
37. Meigs, A.J.; Burbank, D.W.; Beck, R.A.: Middle-late Miocene (> 10 Ma) formation of the Main Boundary thrust in the western Himalaya. *Geology* **23**(5), 423–426 (1995)
38. Iqbal, S.; Jan, I.U.; Akhter, M.G.; Bibi, M.: Palaeoenvironmental and sequence stratigraphic analyses of the Jurassic Datta Formation, Salt Range, Pakistan. *J. Earth Syst. Sci.* **124**(4), 747–766 (2015)
39. Ali, F.; Ahmad, S.; Khan, S.; Hanif, M.; Qiang, J.: Toarcian-Bathonian palynostratigraphy and anoxic event in Pakistan: an organic geochemical study. *Stratigraphy* **15**(3), 225–243 (2018)
40. Khan, S.: *Biostratigraphy and microfacies of the cretaceous sediments in the Indus Basin, Pakistan*. Doctoral Dissertation, University of Edinburgh, Edinburgh, UK (2013)
41. Ullah, A.: *Lithofacies properties, biostratigraphy, cyclicity and depositional environment of the Margala Hill Limestone, Hazara Basin, Northern Pakistan*. Faculty of Graduate Studies and Research, University of Regina (2017)
42. Mughal, M.S.; Zhang, C.; Du, D.; Zhang, L.; Mustafa, S.; Hameed, F.; Khan, M.R.; Zaheer, M.; Blaise, D.: Petrography and provenance of the Early Miocene Murree Formation, Himalayan Foreland Basin, Muzaffarabad, Pakistan. *J. Asian Earth Sci.* **162**, 25–40 (2018)
43. Dunham, R.J.: Classification of carbonate rocks according to depositional texture. In: Ham, W.E. (ed.) *Classification of Carbonate Rocks*. 1st ed. Memoir American Association of Petroleum (1962)
44. Bacelle, L.; Bosellini, A.: Diagrams for visual estimation of percentage composition in sedimentary rocks [Diagrammi per la stima visiva della composizione percentuale nelle rocce sedimentarie]. *Ann. Univ. Ferrara NS sez. IX., Sci. Geol. Paleont.* **1**, 59–62 (1965)
45. Wilson, J.L.: *The Lower Carboniferous Waulsortian Facies*. Carbonate Facies in Geologic History, pp. 148–168. Springer, Berlin (1975)
46. Nizami, A.R.: *Sedimentology of the middle Jurassic Samana Suk Formation in Trans Indus Ranges Pakistan*. Ph.D., University of Punjab, Lahore, Pakistan (2008)
47. Cheema, A.H.: *Microfacies, diagenesis and depositional environments of Samana Suk formation (Middle Jurassic) Carbonates exposed in South East Hazara and Samana Range*. Ph.D., University of the Punjab, Lahore, Pakistan (2010)
48. Scholle, P.A.; Ulmer-Scholle, D.S.: *A color guide to the petrography of carbonate rocks: grains, textures, porosity, diagenesis*. AAPG Memoir 77. America: AAPG (2003)
49. Tucker, M.E.; Wright, V.P.: *Carbonate platforms: facies evolution and sequences*. *Int. Ass. Sed.* **2**, 328 (1990)
50. Davis, R.A.: *Depositional Systems: A Genetic Approach to Sedimentary Geology*. Prentice Hall, Berlin (1983)
51. Adams, A.; MacKenzie, I.: *Carbonate Sediments and Rocks Under the Microscope: A Colour Atlas*. CRC Press, Boca Raton (1998)
52. Alsharhan, A.; Kendall, C.S.C.: Holocene coastal carbonates and evaporites of the southern Arabian Gulf and their ancient analogues. *Earth Sci. Rev.* **61**(3–4), 191–243 (2003)
53. Halley, R.B.; Schmoker, J.W.: High-porosity Cenozoic carbonate rocks of south Florida: progressive loss of porosity with depth. *AAPG Bull.* **67**(2), 191–200 (1983)
54. Miall, A.D.: Whither stratigraphy? *Sed. Geol.* **100**(1–4), 5–20 (1995)
55. Catuneanu, O.; Abreu, V.; Bhattacharya, J.; Blum, M.; Dalrymple, R.; Eriksson, P.; Fielding, C.R.; Fisher, W.L.; Galloway, W.E.; Gibling, M.: Reply to the comments of W. Helland-Hansen on “Towards the standardization of sequence stratigraphy” by Catuneanu et al. [Earth-Sciences Review 92 (2009), pp. 1–33] (2009).
56. Vail, P.R.; Hardenbol, J.; Todd, R.G.: Jurassic unconformities, chronostratigraphy and sea-level changes from seismic stratigraphy and biostratigraphy. In: Schlee, J.S. (ed.) *Interregional Unconformities and Hydrocarbon Accumulation*. American Association of Petroleum Geologists Memoir, pp. 129–144 (1984)
57. Posamentier, H.; James, D.: An overview of sequence-stratigraphic concepts: uses and abuses. In: Posamentier, H. (ed.) *Sequence Stratigraphy and Facies Associations*, vol. 18, pp. 3–18. Blackwell, Oxford (1993)
58. Spence, G.H.; Tucker, M.E.: Modeling carbonate microfacies in the context of high-frequency dynamic relative sea-level and environmental changes. *J. Sediment. Res.* **69**(4), 947–961 (1999)
59. Embry, A.F.; Johannessen, E.P.: Two approaches to sequence stratigraphy. *Stratigr. Timescales* **2**, 85–118 (2017)
60. Haq, B.U.; Hardenbol, J.; Vail, P.R.: Mesozoic and Cenozoic chronostratigraphy and cycles of sea-level changes. In: Wilgus, C.K. et al. (eds.) *Sea-Level Changesóan Integrated Approach* 42, pp. 71–108. SEMP Special Publication, Houston (1988)
61. James, N.P.: *Shallowing-upward sequences in carbonates*. *Facies and Models* (2nd edition) **1**, 213–228 (1984)
62. Wright, V.: Peritidal carbonate facies models: a review. *Geol. J.* **19**(4), 309–325 (1984)
63. Hallam, A.: A review of the broad pattern of Jurassic sea-level changes and their possible causes in the light of current knowledge. *Palaeogeogr. Palaeoclimatol. Palaeoecol.* **167**(1–2), 23–37 (2001)
64. Jacquin, T.; Rusciadelli, G.; Amedro, F.; de Graciansky, P.-C.; Magniez-Jannin, F.: The North Atlantic cycle: an overview of 2nd-Order Transgressive/Regressive Facies Cycles in the Lower Cretaceous of Western Europe (1998)
65. Legarreta, L.; Uliana, M.A.: The Jurassic succession in west-central Argentina: stratal patterns, sequences and paleogeographic evolution. *Palaeogeogr. Palaeoclimatol. Palaeoecol.* **120**(3–4), 303–330 (1996)
66. Surlyk, F.: Sequence stratigraphy of the jurassic-lowermost cretaceous of east greenland (1). *AAPG Bull.* **75**(9), 1468–1488 (1991)
67. Riccardi, A.C.: Scaphitids from the Upper Campanian–Lower Maastrichtian Bearpaw Formation of the western interior of Canada, vol. 354. Geological Survey of Canada (1983)
68. Ahr, W.M.: *Geology of Carbonate Reservoir: The Identification, Description, and Characterization of Hydrocarbon Reservoirs*. Wiley, New York (2008)
69. Warme, J.E.: Jurassic carbonate facies of the central and eastern High Atlas rift, Morocco. In: Jacobshagen, V.H. (ed.) *The Atlas System of Morocco*, pp. 169–199. Springer, Berlin (1988)
70. Ayyıldız, T.; Tekin, E.; Friedman, G.M.: Microtextural properties of ooids in the middle Jurassic-lower Cretaceous, central taurus carbonate platform, Antalya, Turkey. *Carbonates Evaporites* **16**(1), 1–7 (2001)



71. Morettini, E.; Santantonio, M.; Bartolini, A.; Cecca, F.; Baumgartner, P.; Hunziker, J.: Carbon isotope stratigraphy and carbonate production during the Early-Middle Jurassic: examples from the Umbria–Marche–Sabina Apennines (central Italy). *Palaeogeogr. Palaeoclimatol. Palaeoecol.* **184**(3–4), 251–273 (2002)
72. Rousseau, M.; Dromart, G.; Garcia, J.-P.; Atrops, F.; Guillocheau, F.: Jurassic evolution of the Arabian carbonate platform edge in the central Oman Mountains. *J. Geol. Soc.* **162**(2), 349–362 (2005)
73. Gómez, J.; Fernández-López, S.R.: The Iberian Middle Jurassic carbonate-platform system: synthesis of the palaeogeographic elements of its eastern margin (Spain). *Palaeogeogr. Palaeoclimatol. Palaeoecol.* **236**(3–4), 190–205 (2006)
74. Čadjenović, D.; Kilibarda, Z.; Radulović, N.: Late Triassic to Late Jurassic evolution of the Adriatic carbonate platform and Budva Basin, southern Montenegro. *Sed. Geol.* **204**(1–2), 1–17 (2008)
75. Delmas, J.; Brosse, E.; Houel, P.: Petrophysical properties of the middle Jurassic carbonates in the PICOREF sector (South Champagne, Paris Basin, France). *Oil Gas Sci. Technol. Revue de l'Institut Français du Pétrole* **65**(3), 405–434 (2010)
76. Han, Z.; Hu, X.; Li, J.; Garzanti, E.: Jurassic carbonate microfacies and relative sea-level changes in the Tethys Himalaya (southern Tibet). *Palaeogeogr. Palaeoclimatol. Palaeoecol.* **456**, 1–20 (2016)
77. Alsharhan, A.; Nairn, A.: The Late Permian carbonates (Khuff Formation) in the western Arabian Gulf: its hydrocarbon parameters and paleogeographical aspects. *Carbonates Evaporites* **9**(2), 132 (1994)
78. Alsharhan, A.S.; Magara, K.: Nature and distribution of porosity and permeability in Jurassic carbonate reservoirs of the Arabian Gulf Basin. *Facies* **32**(1), 237–253 (1995)
79. Nairn, A.; Alsharhan, A.: *Sedimentary Basins and Petroleum Geology of the Middle East*. Elsevier, Berlin (1997)
80. Sudarsana, A.; Abdelouahab, M.; Chanpong, R.; Fryer, V.I.; Hall, J.; Vizcarra, E.: A Mid-Jurassic carbonate reservoir case study, Offshore Qatar: how to capture high permeable streaks in a 3D reservoir model. In: *International Petroleum Technology Conference 2009*. International Petroleum Technology Conference

